Body-centred-cubic (BCC) lattice model of nuclear structure

Gamal A. Nasser
Faculty of science, Mansoura University, Egypt.
E-mail: chem.gamal@hotmail.com.

Abstract:

This model is development of solid nuclear models. Like FCC model, this model can account for nuclear properties that have been explained by different models. This model gives more accurate explanation for some nuclear properties which are Asymmetric fission, Nuclear binding energy and the most bound nuclei, Natural radioactivity and Number of neutrons in nuclei depending on the structures of these nuclei. The structures of nuclei in this model have special advantage, as there is separation between lattice positions of similar nucleons giving new concept for nuclear force.

1. INTRODUCTION

Physics dealt with the atomic nucleus and there were number of nuclear models suggested by scientists to account for the nuclear properties and the manner by which protons and neutrons exist in the nucleus. Each of these models succeeded to account for certain selected properties of the nucleus but failed to account for other properties.

A. There are three basic nuclear models

- Cluster model:
  It proposes that nucleus is a cluster of alpha particles. The main property that cluster model accounts for is the alpha decay. [1]

- Liquid drop model:
  It proposes that nucleons exist in nucleus like molecules in liquid drop. The properties that liquid drop model could account for are the constancy of nuclear density consequently, the nuclear radius, also the nuclear binding energy and the fission process, but could not account for asymmetrical fission. [2]

- Shell model:
  It proposes that nucleons exist in gaseous state. The main property that shell model accounts for is stability of nuclei which have certain numbers of protons or neutrons called magic numbers. [3]

These developed models, shell, liquid drop and cluster, assume a gas, liquid and semi-solid phase for the nucleus respectively. The comprehensive description of the nucleus; therefore, most likely should come from a model representing a different phase. The remaining phase left is solid. [4]

B. Solid phase nucleus model

In the last few decades scientists started to direct their research to account for a solid nucleus model.
Solid phase has not been considered as a viable option for many decades because of the uncertainty principle and the lack of diffraction. In the 1960s the discovery of quarks and neutron star researches satisfactorily answered these objections and opened the door for solid nuclear structures. The proposed models assume that

the protons and the neutrons have same size; the individual nucleon has a spherical shape; protons and neutrons are alternating; and the nucleons are arranged in a close packing crystal structure. These assumptions are reasonable. The radii of protons and the neutrons differ only slightly. [5]
The main property that solid phase model accounts for is the asymmetrical fission.

C. Face-centred-cubic (FCC) Lattice Model of Nuclear Structure *by Norman D. Cook.* [8]

This model considered nucleons to have FCC lattice structure. This solid phase model was directed to account for nuclear properties that have been explained by different models like:

- Constancy of nuclear density, nuclear fission, depending of nuclear radius on A and saturation of nuclear force for liquid drop model.
- It gave relationship between lattice positions of nucleons and quantum number in shell model.
- It also dealt with nucleus as alpha particles constructed body.
- Also this model gave some explanation for asymmetric fission.

2. BODY-CENTERED-CUBIC (BCC) LATTICE MODEL OF NUCLEAR STRUCTURE

This model can account for many nuclear properties like FCC model, but this model gives more accurate explanation for

- Asymmetric fission and its products.
- Nuclear binding energy and gives a new formula for calculating it.
- Other nuclear properties.

The main advantage of the **shapes** of nuclei in BCC model is that **(the distance between the identical nucleons will be much bigger than the distance between unlike nucleons and these distances will be kept constant in any nucleus).** This advantage also exists in Simple Cubic lattice.
It is clear that this shape (figure 2.1) gives the mentioned advantage, but it is a planner shape.

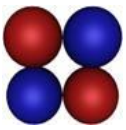

Figure 2.2.

So what is real shape of alpha particle?
The real shape of alpha particle (The BCC lattice) (Figure 2.2)
Two opposite sides of the square rotate on each other until we reach the real shape of alpha particle which will be **two identical triangles shared in base and perpendicular on each other.**

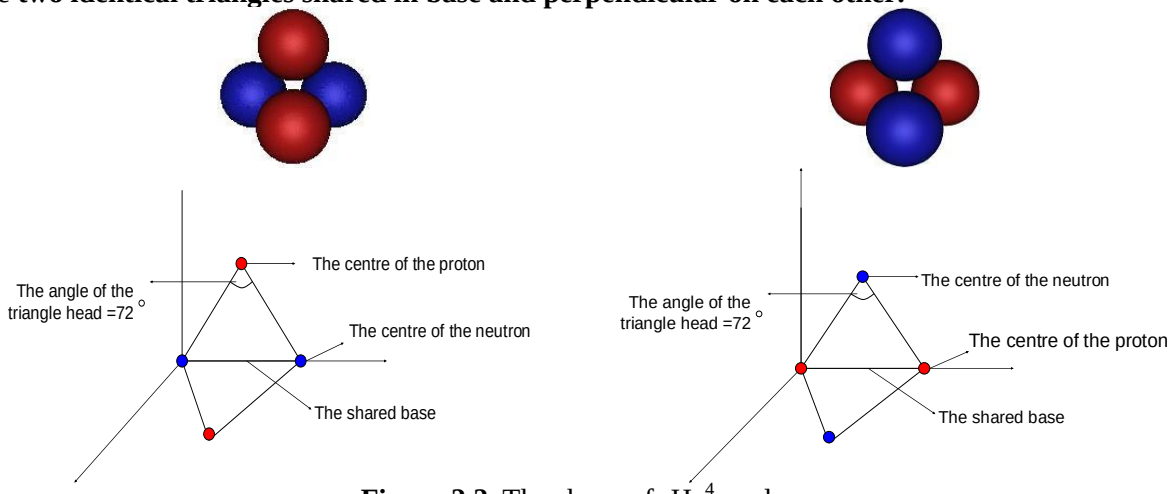

Figure 2.2. The shape of $_2He^4$ nucleus.

Note:* The two shapes are the same one but only rotated.
** The distances are calculated from the centres of nucleons.

Calculations: in these calculations it is considered that the radius of proton equals 1.2 fm. [9] and it is considered that the radius of neutron equals this value.

1- Any side of the two triangles = the radius of a proton + the radius of a neutron
=1.2 fm + 1.2 fm = 2.4 fm

2-The distance between two identical nucleons **(R)** = the length of the shared base

$$\mathbf{(R)} = [(2.4)^2 + (2.4)^2 + \mathbf{(}2 \times 2.4 \times 2.4 \times \cos(72)\mathbf{)}]^{1/2} = 2.82137 \text{ fm.}$$

This distance between two similar nucleons in alpha particle is constant between any two adjacent similar nucleons in all heavier nuclei.
This assumed shape of alpha particle will be the structural unit of the shapes of all nuclei.

3. SHAPES OF NUCLEI IN BCC MODEL

All nuclei tend to take **spherical shape** because it has the lowest surface tension and nucleons are bounded to maximum number of neighbours. The following presentation of the shapes of nuclei will depend on the positions available by previous shapes. It is **not a presentation of synthetic pathway** for nuclei but it is only a way for suggesting the structures of nuclei tending to be close to spherical shapes.

A. The shape of $_3Li^7$ nucleus. (Figure 3.1)

The 1P and 2_0n^1 will take the shape of a triangle identical to the two triangles of alpha particle and this triangle apply up sided down to one of the two triangles as the added proton applies to the neutron base.

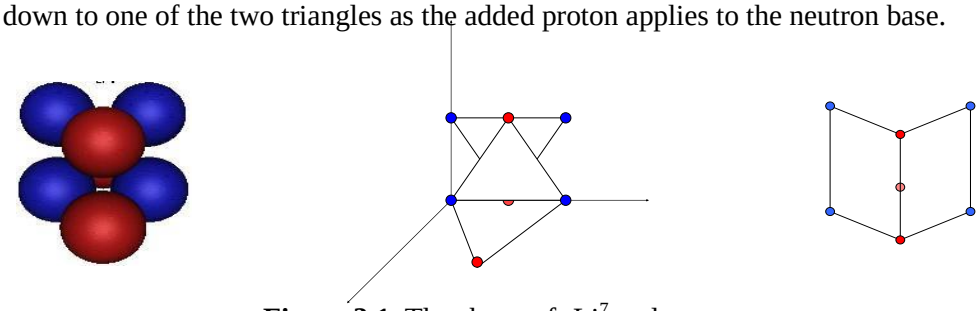

Figure 3.1. The shape of $_3Li^7$nucleus.

Alpha particle makes with the two added neutron a shape of two parallelograms shared in one side and they are not in the same plane so the next addition is a D nucleus as the proton will be added to the two neutrons base and the neutron will be added to the two proton base.

B. The shapes of $_4Be^9$and $_5B^{11}$ (Figure 3.2), (Figure 3.3).

$_4Be^9=_3Li^7 +1P +1_0n^1$
The proton and the neutron are added on one of the two parallelograms of $_3Li^7$ nucleus.

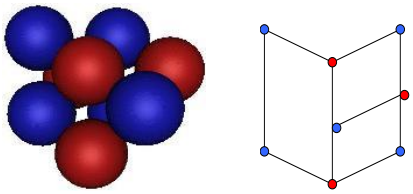

Figure 3.2. The shape of $_4Be^9$nucleus.

$_5B^{11}= _4Be^9+ 1P +1_0n^1$
By the same previous mechanism.

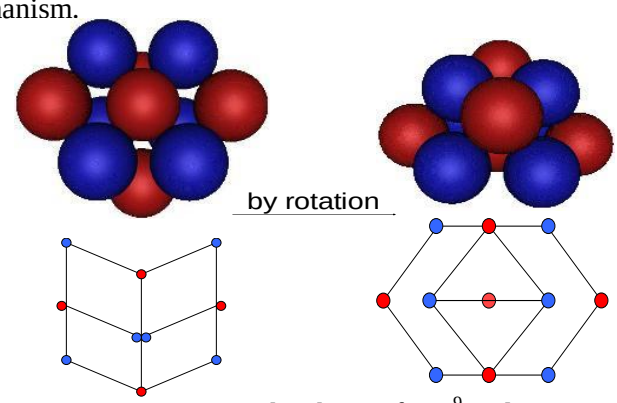

Figure 3.3. The shape of $_4Be^9$nucleus.

It is clear that $_5B^{11}$ nucleus has a base take the shape of a hexagon and formed from 3p and 4_0n^1also it has a peak takes a shape of two identical triangles shared in base and they are in the same plane and formed from 2p and 2_0n^1. This peak represents the complete addition to the hexagon base as it can not receive any other nucleons on the face in front of us.

If we make an addition to the hexagon it will be $1P + 2_0n^1$ and to complete the addition to it we need only one proton. (Figure 3.4), (figure 3.5), (figure 3.6)

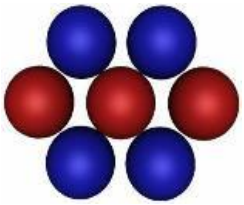

Figure 3.4. The hexagon.

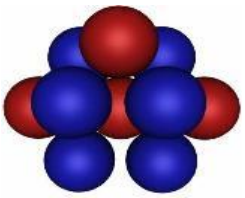

Figure 3.5. First addition.

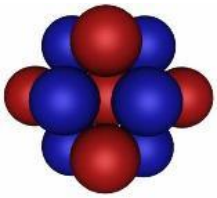

Figure 3.6. Second addition.

C. The shape of $_6C^{12}$nucleus

$_6C^{12} = {}_5B^{11} + 1P$

This addition was expected to be on the other face of the hexagon, but there is only one proton added and the hexagon receives **T** nucleus in the first addition so this addition will be on the two neutron of the peak.

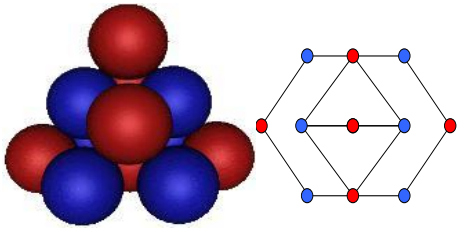

Figure 3.7. The shape of $_6C^{12}$nucleus.

3. TYPE A AND TYPE B SHAPES OF NUCLEI.

It's noted that nuclei in which Z = N can give the same shape by substituting the positions of protons by neutrons and vice versa.

A. The two shapes of $_6C^{12}$ nucleus

The first shape of $_6\mathbf{C}^{12}$nucleus (Figure 4.1.A.) and the shapes of nuclei which will grow from this first shape are considered to be **type A** shapes. In the same way the second shape of $_6\mathbf{C}^{12}$nucleus (Figure 4.1.B.) and nuclei which will grow from it are considered to be **type B** shapes.

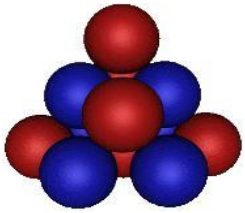

Figure 4.1.A.

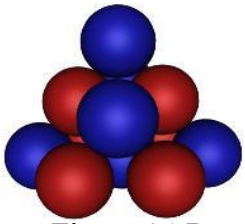

Figure 4.1.B.

B. The two shapes of $_8O^{16}$ nucleus.

One of the two shapes will be the growth of type A $_6\mathbf{C}^{12}$nucleus (Figure 4.2.A.) and the other will be the growth of type B $_6\mathbf{C}^{12}$nucleus (Figure 4.2.B.).

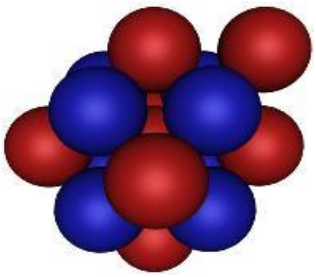

Figure 4.2.A.

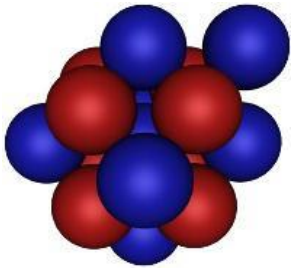

Figure 4.2.B.

C. The two shapes of $_{10}Ne^{20}$ nucleus. (Figure 4.3.A.), (Figure 4.3.B.).

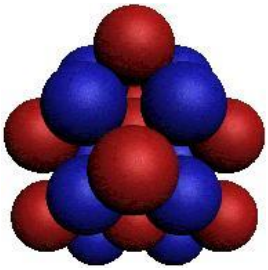

Figure 4.3.A.

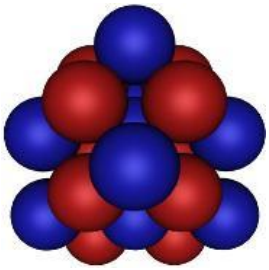

Figure 4.3.B.

D. The two shapes of $_{12}Mg^{24}$ nucleus. (Figure 4.4.A.), (Figure 4.4.B.).

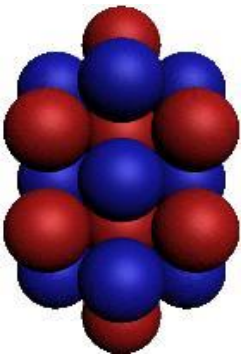

Figure 4.4.A.

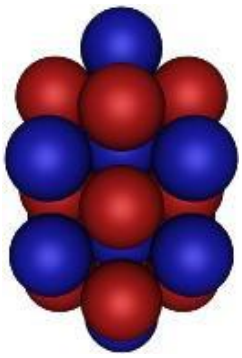

Figure 4.4.B.

Type A $_{12}Mg^{24}$ will grow from four side giving $_{20}Ca^{40}$ nucleus but type B $_{12}Mg^{24}$ will grow from only one side giving the same shape of $_{20}Ca^{40}$ nucleus as this shape of $_{20}Ca^{40}$ nucleus is the only one which can grow to spherical shapes of heavier nuclei.

5. THE GROWTH OF TYPE A $_{12}Mg^{24}$ FROM FOUR SIDES

It explains why from $_{12}Mg^{24}$ to $_{20}Ca^{40}$ nuclei which have odd number of protons have one excess neutron as $_{12}Mg^{24}$ is formed from four hexagons and the suitable additions to these hexagons explains number of neutrons in these nuclei as the first addition to a hexagon is 1P and 2_0n^1 giving nuclei with one excess neutron.

A. The shapes of $_{13}Al^{27}$ and $_{14}Si^{28}$ nuclei. (Figure 5.1.), (Figure 5.2.)

These two additions will be on one of the four vertical hexagons of $_{12}Mg^{24}$ nucleus so they will take the mechanism of addition to hexagons

$_{13}Al^{27} = {}_{12}Mg^{24} + 1P + 2_0n^1$

$_{14}Si^{28} = {}_{13}Al^{27} + 1P$

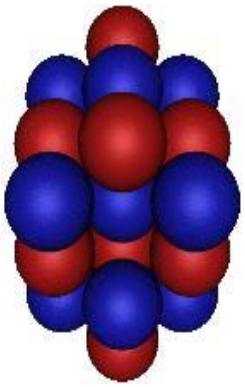

Figure 5.1. The shape of $_{13}Al^{27}$ nucleus.

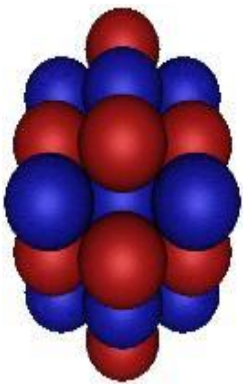

Figure 5.2. The shape of $_{14}Si^{28}$ nucleus.

B. The shapes of $_{15}P^{31}$ and $_{16}S^{32}$ nuclei. (Figure 5.3.), (Figure 5.4.)

These two additions will be on the opposite vertical hexagon.

$_{15}P^{31} = {}_{14}Si^{28} + 1P + 2{}_0n^1$

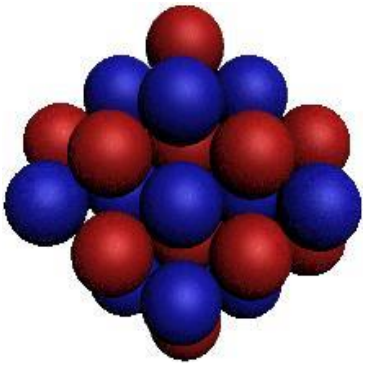

Figure 5.3. The shape of $_{15}\mathbf{P^{31}}$ nucleus.

$_{16}S^{32} = {}_{15}P^{31} + 1P$

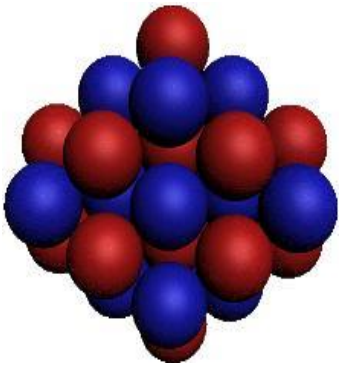

Figure 5.4. The shape of $_{16}\mathbf{S^{32}}$ nucleus.

C. The shapes of $_{17}Cl^{35}$ and $_{18}Ar^{36}$ nuclei. (Figure 5.5.), (Figure 6.6.)

$_{17}Cl^{35} = {}_{16}S^{32} + 1P + 2{}_0n^1$

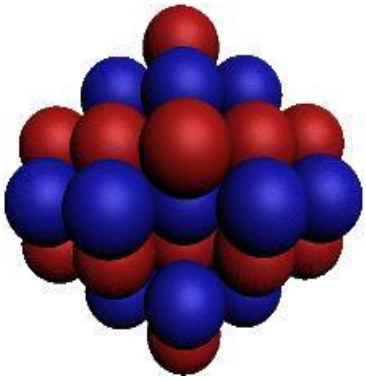

Figure 5.5. The shape of $_{17}\mathbf{Cl^{35}}$ nucleus.

$_{18}Ar^{36} = {}_{17}Cl^{35} + 1P$

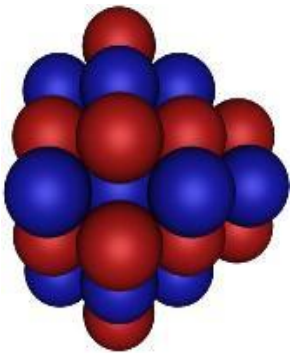

Figure 5.6. The shape of $_{18}\mathbf{Ar^{36}}$ nucleus.

D. The shapes of $_{19}k^{39}$ and $_{20}Ca^{40}$ nuclei. (Figure 5.7.), (Figure 5.8.)

$_{19}k^{39} = {}_{18}Ar^{36} + 1P + 2{}_0n^1$

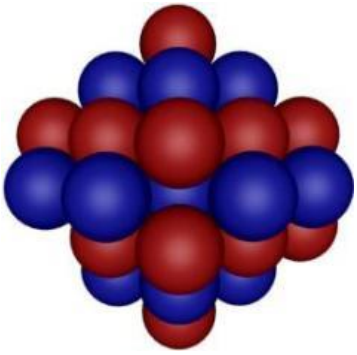

Figure 5.7. The shape of $_{19}\mathbf{k^{39}}$ nucleus.

$_{20}Ca^{40} = {}_{19}k^{39} + 1P$

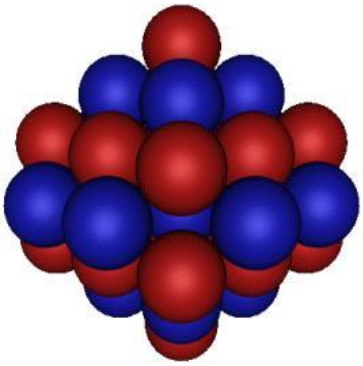

Figure 5.8. The shape of $_{20}\mathbf{Ca^{40}}$ nucleus.

6. THE GROWTH OF TYPE B $_{12}Mg^{24}$ FROM ONE SIDE.

This shape of $_{12}\mathbf{Mg^{24}}$ grows from only one side giving the same shape of $_{20}\mathbf{Ca^{40}}$ nucleus as this shape of $_{20}\mathbf{Ca^{40}}$ nucleus is the only one which can grow to spherical shapes of heavier nuclei.

A. The shape of $_{18}Ar^{38}$ and $_{18}Ar^{40}$ nuclei. (Figure 6.1.), (Figure 6.2.)

Complete addition on this side make it grows forming $_{18}\mathbf{Ar}^{38}$ then by adding two protons it gives the same shape of $_{20}\mathbf{Ca}^{40}$ nucleus.

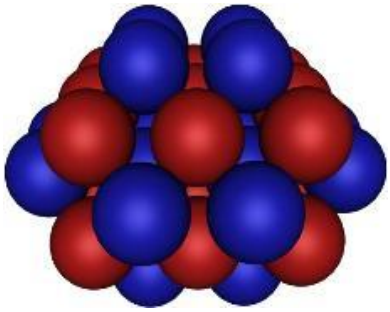

Figure 6.1. The shape of $_{18}\mathbf{Ar}^{38}$ nucleus.

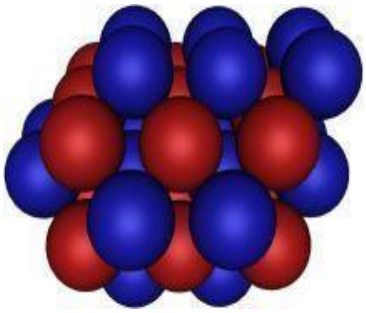

Figure 6.2. The shape of $_{18}\mathbf{Ar}^{40}$ nucleus.

B. The shape of $_{20}\mathbf{Ca}^{40}$ nucleus. (Figure 6.3.)

$_{20}Ca^{40}$ is formed of two identical pyramids separated by neutrons layer. The growth will be from one pyramid until $_{28}Ni^{60}$.

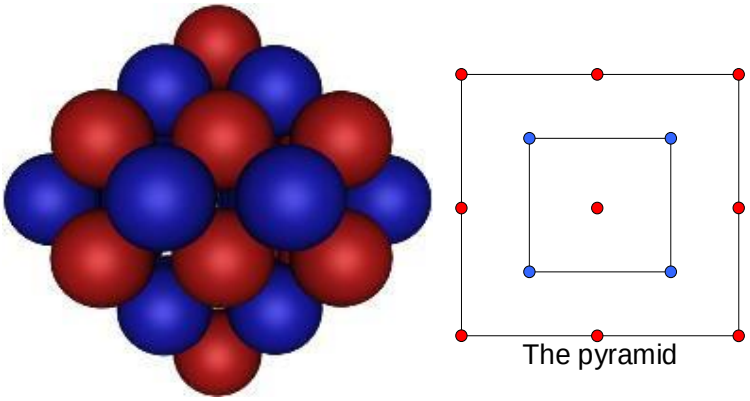

Figure 6.3. The shape of $_{20}\mathbf{Ca}^{40}$ nucleus.

C. The shape of $_{28}\mathbf{Ni}^{60}$ nucleus. (Figure 6.4.)

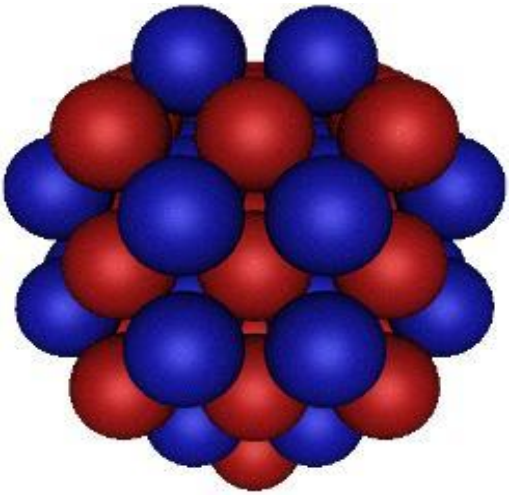

Figure 6.4. The shape of $_{20}\mathbf{Ca}^{40}$ nucleus.

Ni and **Co** nuclei have in this structure the closest shapes to a perfect spherical shape. **Fe, Co** and **Ni** have the highest nuclear binding energy per nucleon and lie on the top of the nuclear binding energy curve and this will be discussed later. All nuclei until **Fe** and **Ni** are formed by nuclear fusion releasing energy nuclei after that are formed by absorption of energy.

7. The shapes of heavy nuclei after Ni.

These nuclei are formed by addition of protons layers tending to have spherical shapes. There will be nuclei in which protonic skeleton is formed of complete layers **(Kr - Cd - Gd - Hg).**

A. The shape of $_{36}Kr^{84}$ nucleus.

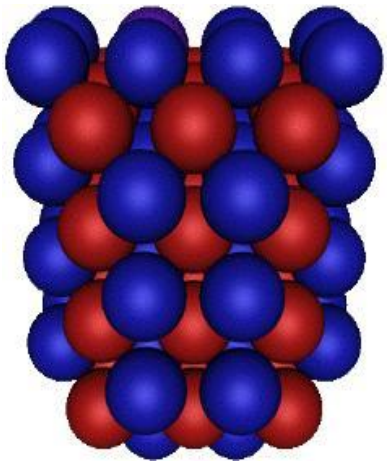

Figure 7.1. The shape of $_{36}Kr^{84}$ nucleus.

B. The shape of $_{48}Cd^{114}$ nucleus.

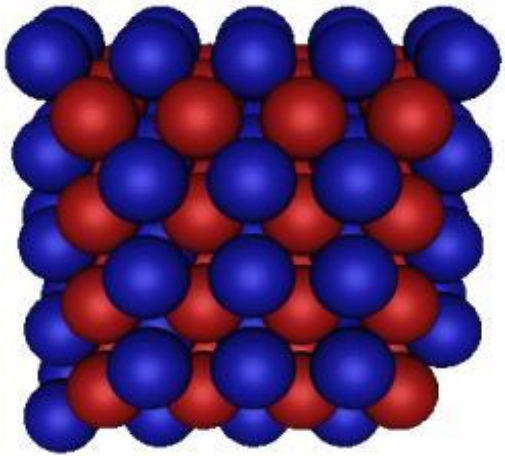

Figure 7.2. The shape of $_{48}Cd^{114}$ nucleus.

C. The shape of $_{56}Ba^{138}$ nucleus.

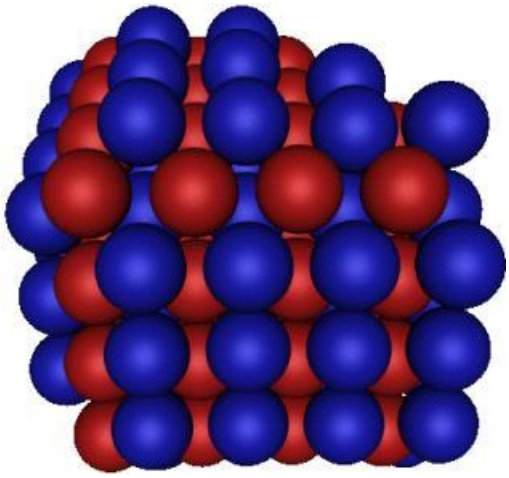

Figure 7.3. The shape of $_{56}Ba^{138}$ nucleus.

D. The shape of $_{64}Gd^{158}$ nucleus.

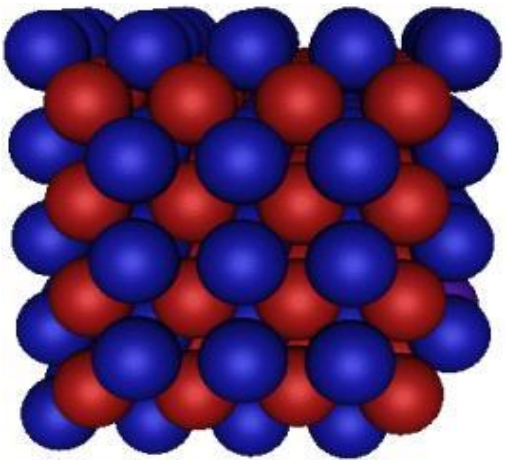

Figure 7.4. The shape of $_{64}Gd^{158}$ nucleus.

E. The shape of $_{80}Hg^{202}$ nucleus.

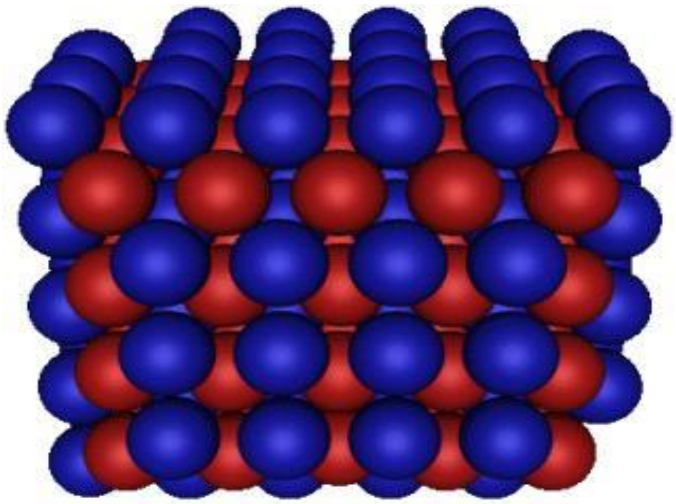

Figure 7.5. The shape of $_{80}Hg^{202}$ nucleus.

F. The shape of $_{92}U^{238}$ nucleus.

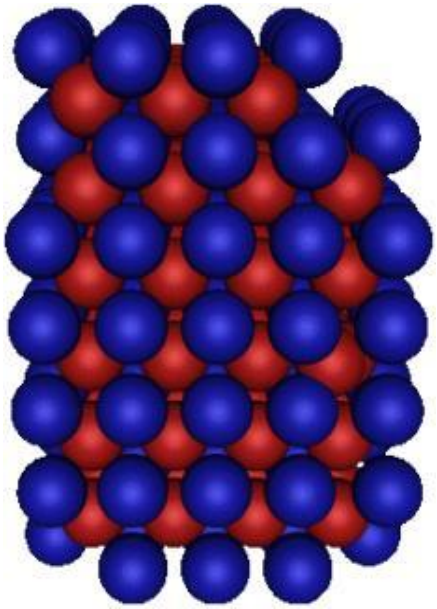

Figure 7.6. The shape of $_{92}U^{238}$ nucleus.

8. THE BINDING ENERGY IN BCC MODEL.

In this model every nucleon is surrounded by number of unlike nucleons as a proton is surrounded by number of neutrons and vice versa. The maximum number of neighbours for each nucleon is 8 nucleons.
(As every nucleon makes bonds with its neighbours, the number of bonds for a nucleus equals the sum of bonds between nucleons.)

A. Number of bonds for nucleus.

Number of bonds in each nucleus is calculated and listed in table 1. **Appendix A**
By plotting mass number versus number of bonds per nucleon (Figure 8.1) it was found that there is saturation occurs after atomic mass around 60. This saturation is similar to saturation of binding energy so there is a relation between number of bonds in a nucleus and its binding energy.
Note : Number of bonds in heavy nuclei after Ni may differ by one or two in some nuclei because there are number of possibilities for nuclei shapes except in nuclei in which protonic skeleton is formed of complete layers (Kr - Cd - Gd - Hg).

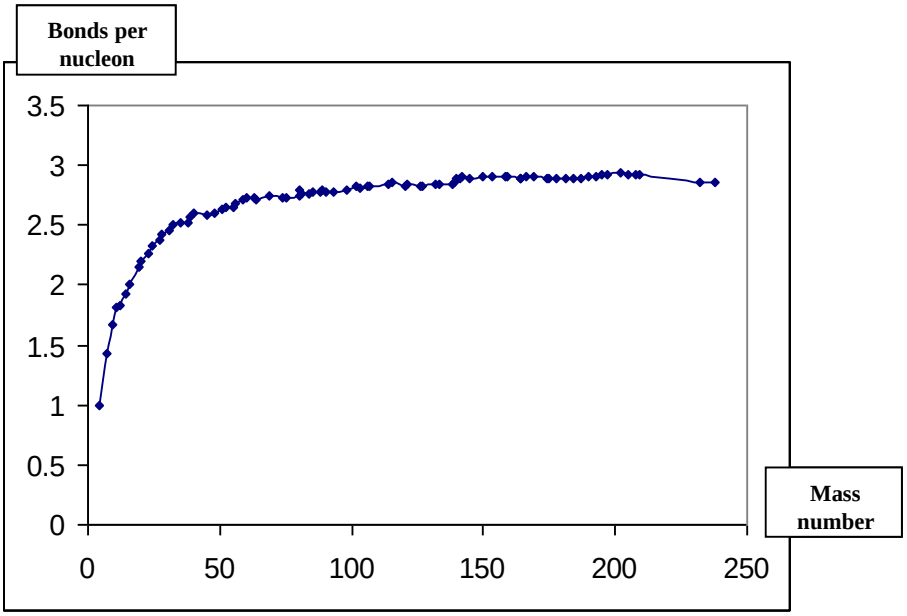

Figure 8.1. Plot of mass number versus number of bonds per nucleon.

B. Relation between number of bonds and binding energy

As mentioned above binding energy of a nucleus is proportional to number of bonds **(B)** in this nucleus

$$E_b \propto B$$

$$E_b = \text{cons } B - \text{Coulomb repulsion of the protons}$$

$$\text{Constant} = \left(E_b + (0.711_{(MeV)}\, Z^2) / A^{1/3}\right) / B$$

By plotting sum $\left(E_b + (0.711_{(MeV)}\, Z^2) / A^{1/3}\right)$ versus **B** (Figure 8.2). Table 2. (**Appendix B)**. It gives almost straight line as the slope is the constant. There is deviation in lighter nuclei as it gives slight higher values for constant and it is because these nuclei have lower value for number of bonds per nucleon.

$$\text{Slope} = \left(E_b + (0.711_{(MeV)}\, Z^2) / A^{1/3}\right) / B$$
$$= 4.08 \text{ MeV}$$

The new formula for calculating binding energy.

$$E_b = 4.08_{(MeV)}\, B - (0.711_{(MeV)}\, Z^2) / A^{1/3}$$

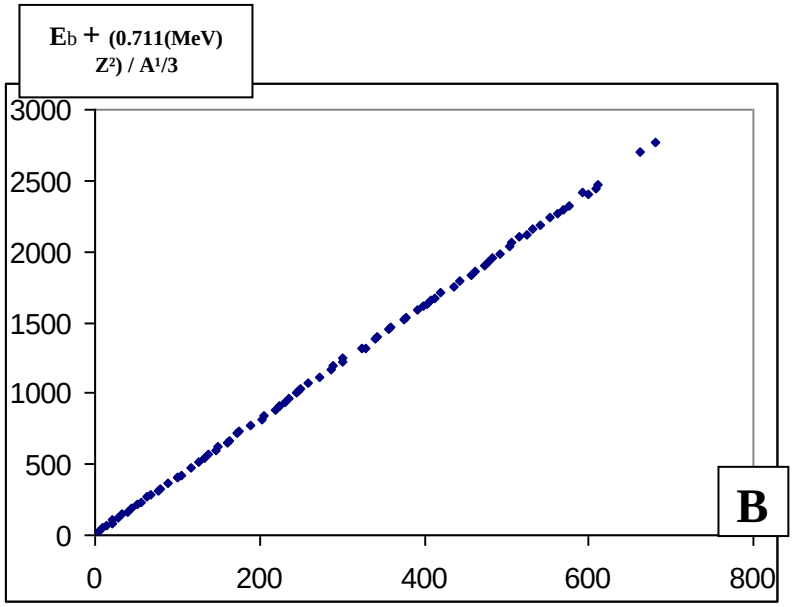

Figure 8.2. Plot of number of bonds (B) versus sum.

C. Results of using the new formula

1- This model by this formula is the only model which can give explanation for binding energy of any nucleus depending on its structure.

2- This model also gives explanation for elements which have the highest nuclear binding energy per nucleon and lie on the top of the nuclear binding energy curve as
   - **Fe, Co** and **Ni** have in this model the closest shapes to a perfect **spherical shape** so these nuclei have small surface area allowing their nucleons to have more binding energy.
   - Nearly there is a saturation of number of bonds per nucleon after **Ni** as the increase of the value of **B** per nucleon after **Ni** is very small and it's opposed by higher increase in the coulomb effect.
   - This spherical shape and this level of saturation are the accurate explanation of this phenomenon.

3- Bonds in this model represent interaction between unlike nucleons (a proton and a neutron) so if it is assumed that the constant in formula represents the energy of each bond, this may give a new concept of the nuclear force. (Section 12.)

9. ASYMMETRIC FISSION IN BCC MODEL.

BCC model gives very accurate explanation for asymmetric fission and the difference between the products in atomic mass.

A. The puzzle of asymmetric fission.

Vandenbusch and Huizenga (1973, p. 259) : "Asymmetric mass distributions have proved to be one of the most persistent puzzles in the fission process… [N]o theoretical model has been generally accepted… The most significant failure of the [liquid-drop] theory is the failure to account for asymmetric mass distributions…
Moreau and Heyde (1991, p. 228): "The theoretical description of the fission process ... is one of the oldest problems in nuclear physics… it appears that a consistent description of fission is still very far away."

B. Fission process

Fission process undergo according to this equation

$$_{92}\mathbf{U}^{235} + {}_{0}\mathbf{n}^{1} = {}_{56}\mathbf{Ba}^{141} + {}_{36}\mathbf{Kr}^{92} + 3{}_{0}\mathbf{n}^{1}$$

As $_{56}\mathbf{Ba}^{141}$ and $_{36}\mathbf{Kr}^{92}$ represents two isotopes which are from the major products of fission process.
This model gives accurate explanation for fission process depending on the structure of the fissionable nucleus and its products.

If we review the protonic structure of nuclei in the previous equation, we will find obvious relation between the fissionable nucleus and its products. (Figure 9.1), (Figure 9.2), (Figure 9.3.)

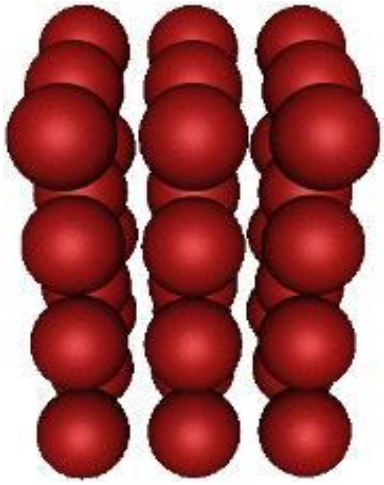

Figure 9.1. The protonic skeleton of **Kr**.

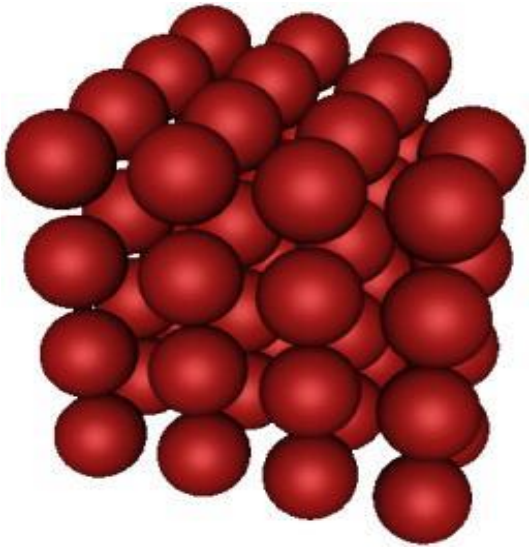

Figure 9.2. The protonic skeleton of **Ba.**

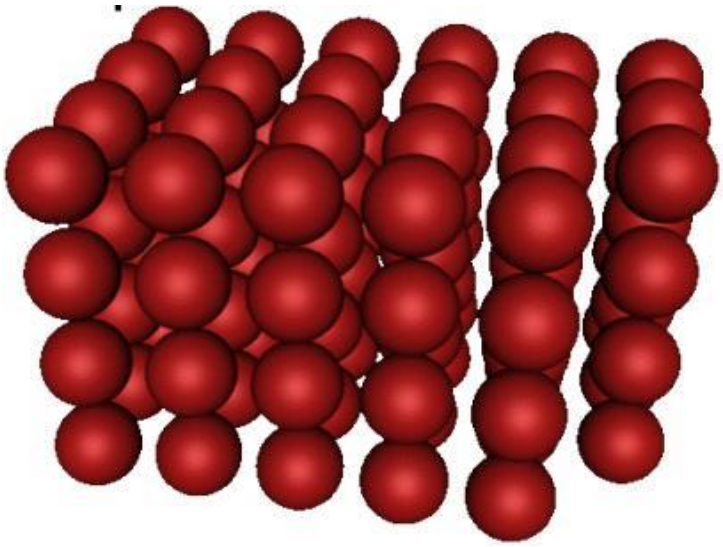

Figure 9.4. The protonic skeleton of **U**.

It is clear that U skeleton can be divided into the skeleton of Kr and skeleton very close to Ba which can regain its original shape very easily. (Figure 9.4), (Figure 9.5).

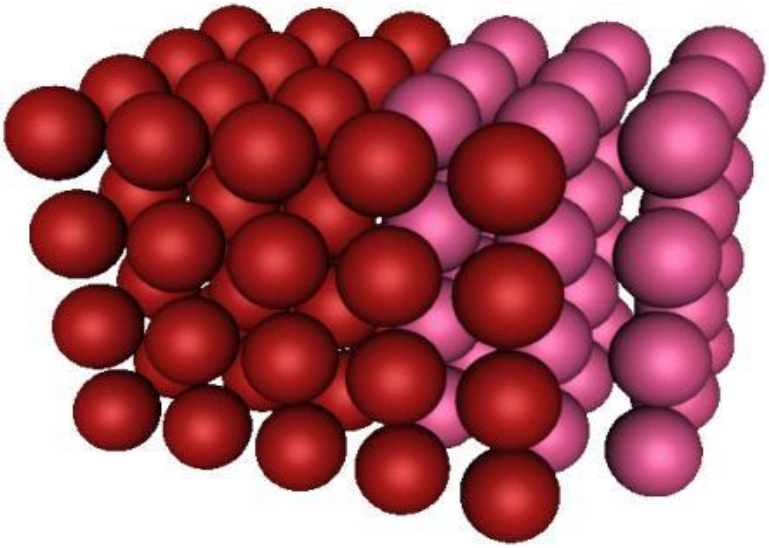

Figure 9.3. skeleton of **U** = skeleton of Kr + Ba.

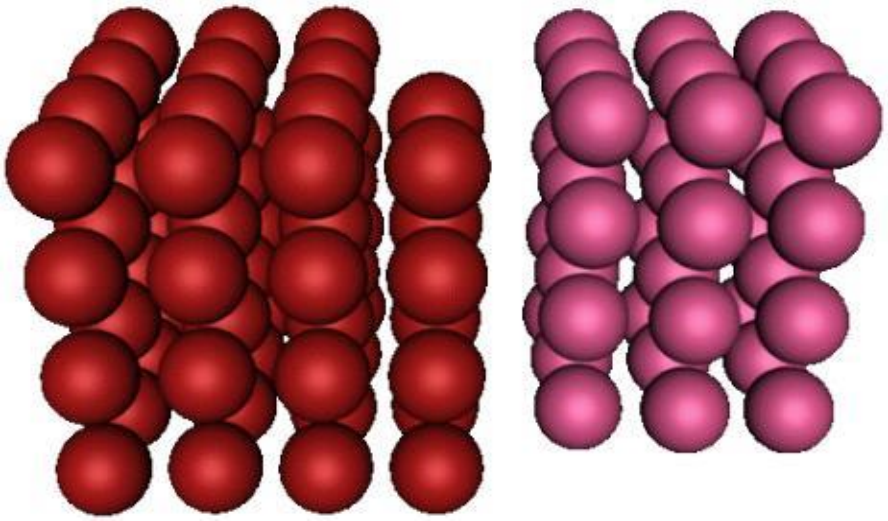

Figure 9.5. U fission gives Ba and Kr.

$$_{92}\mathbf{U}^{235} + {}_{0}\mathbf{n}^{1} = {}_{56}\mathbf{Ba}^{141} + {}_{36}\mathbf{Kr}^{92} + 3{}_{0}\mathbf{n}^{1}$$

This equation can be represented by (Figure 9.6), (Figure 9.7), (Figure 9.8.)

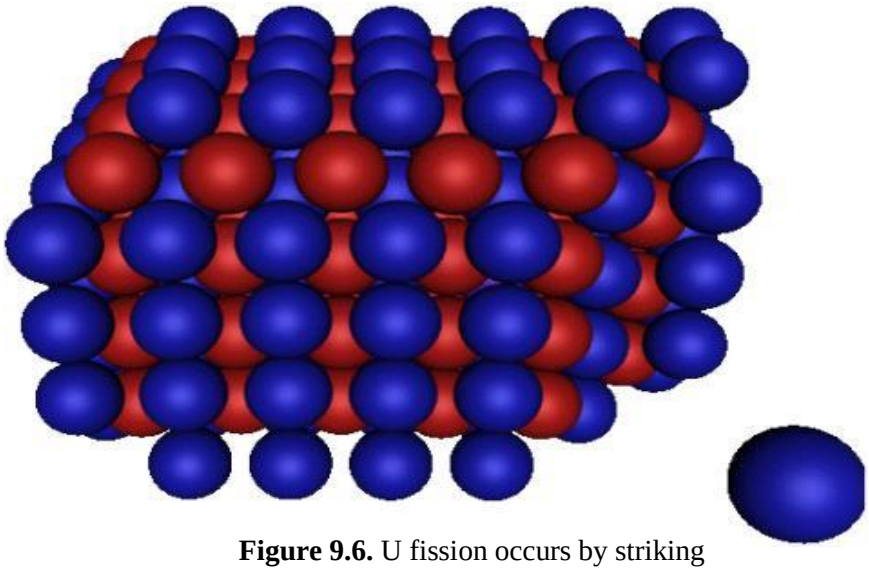

Figure 9.6. U fission occurs by striking
U nucleus by a neutron.

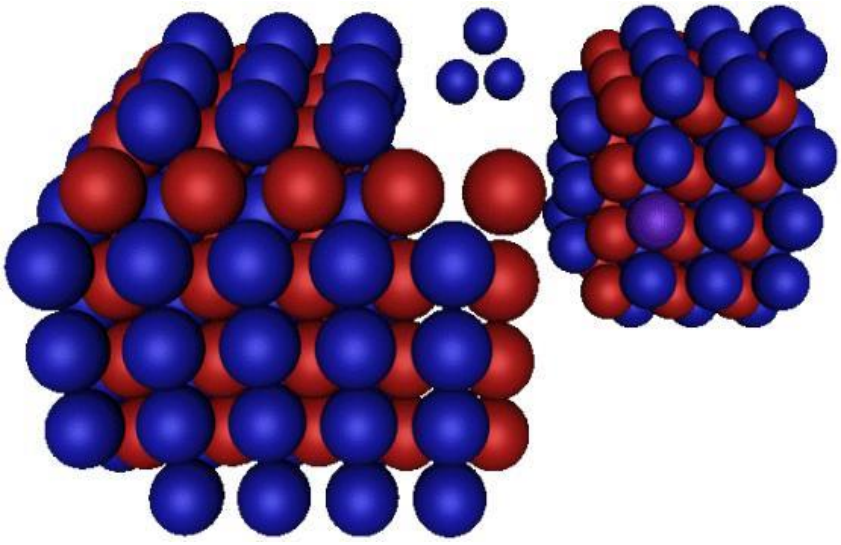

Figure 9.7. $_{92}\mathbf{U}^{235}$ fission gives $_{36}\mathbf{Kr}^{92}$ And $_{56}\mathbf{Ba}^{141}$

But $_{56}$**Ba**^{141}differs slightly from its original shape.

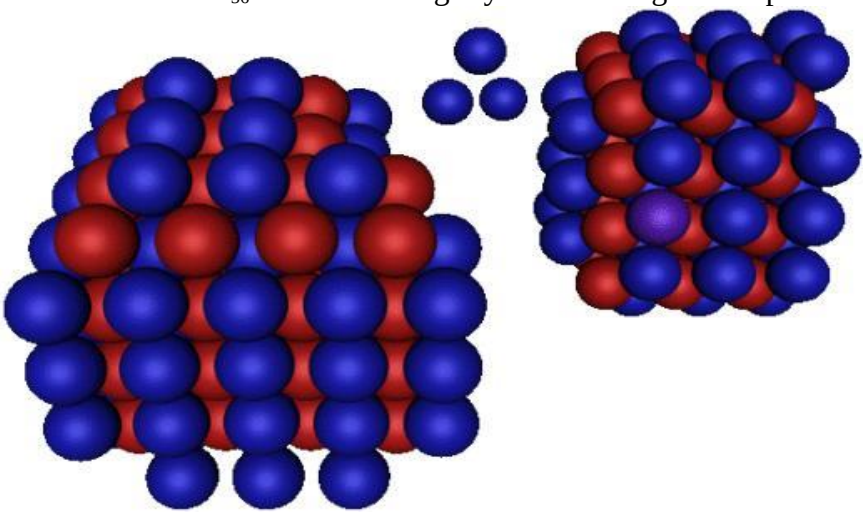

Figure 9.8. $_{56}$**Ba**^{141}can easily regain its original shape.

C. This is the most accurate explanation for asymmetric fission as

1- The structure of $_{92}$**U**^{235} expects accurately the fission products.

2- The plane from which U skeleton can be divided gives range of structures from (**Kr** to **Ru**) and respectively from (**Ba** to **Cd**) also by surpassing this plane it can give nuclei slightly heavier than **Ba** and lighter than **kr**. This range of products agrees to high level with experimental results of fission products.

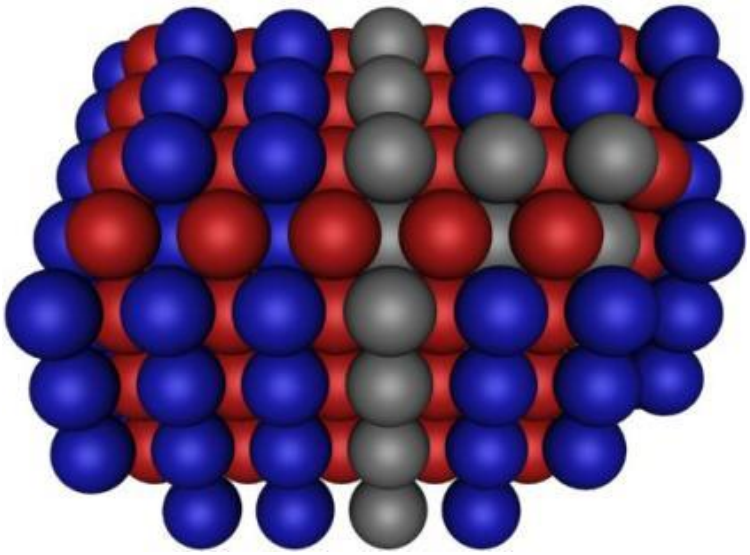

Figure 9.9. $_{92}$**U**^{235} fission gives $_{36}$**Kr**^{92} And $_{56}$**Ba**^{141}

Also this plane can be considered a plane of symmetrical fission as it divide **U** nucleus from the side at which there are complete layers of protons into two symmetric parts (only from this side).

3- As this is a solid model so if there is difference between the original shapes of lighter nuclei and their shapes which produced from a sample fission, there will be difference in number of bonds in each shape so there will be difference in energy of each shape.
Consequently the structure of the fissionable nucleus must consist of the structures of fission products or structures very close to original ones to be easy for them to regain their original structures without change in energy.

4- Except In **U** nucleus and nuclei close to it like **Pu**, all structures of nuclei in this model cannot be divided into structures of lighter nuclei with out difference between the original shapes of these lighter nuclei structures and their shapes which produced from division. This can be quite reasonable explanation that **U** and close elements are the common fissionable nuclei.

5- If it is assumed that in fission process neutron strike U nucleus from the incomplete side, this can be an explanation that $_{92}\mathbf{U}^{238}$ is not a fissionable nucleus and $_{92}\mathbf{U}^{235}$ and $_{94}\mathbf{Pu}^{239}$ are fissionable ones.
The incomplete side of $_{92}\mathbf{U}^{235}$ nucleus has an exposed line of protons (Figure 9.9) which can receive neutrons so the neutron can strike at this line. In contrast this line of protons is covered by neutrons in $_{92}\mathbf{U}^{238}$ nucleus (Figure 9.10). $_{94}\mathbf{Pu}^{239}$ nucleus regains two exposed protons at this line (Figure 9.11.) which can receive neutron.

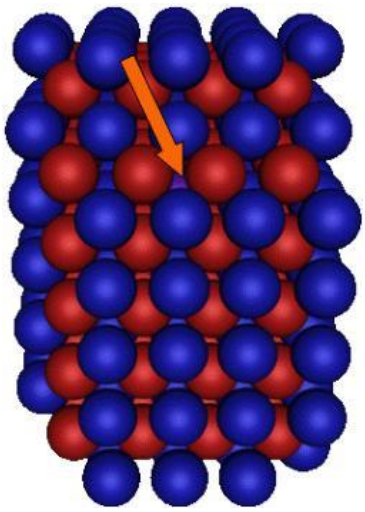

Figure 9.9.

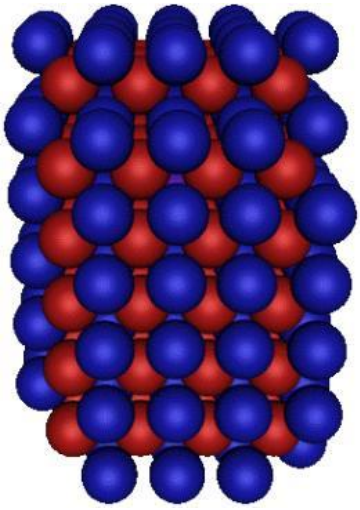

Figure 9.10.

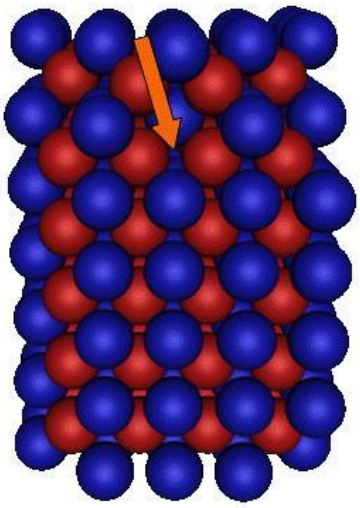

Figure 9.11.

10. RADIOACTIVE DECAY AND ALPHA CLUSTER PROPERTIES IN BCC MODEL

In this model the structural units can be considered alpha particles and the surface of each nucleus is formed of these alpha particles and this can explain alpha decay.
This model gives a new concept for the reason that natural radioactive decay ends with **Pb** and **Bi** as nuclei after **Hg** in this model are considered deviations from spherical shape. The layer of nucleons added after **Hg** should have been on the bigger side to grow forming a spherical shape, but they are added to smaller side deviating from spherical shape so the structure tends to lose this layer to obtain a shape can grow forming a spherical shape. Losing this layer occurs by alpha decay ending by **Pb** which is very close to **Hg**.

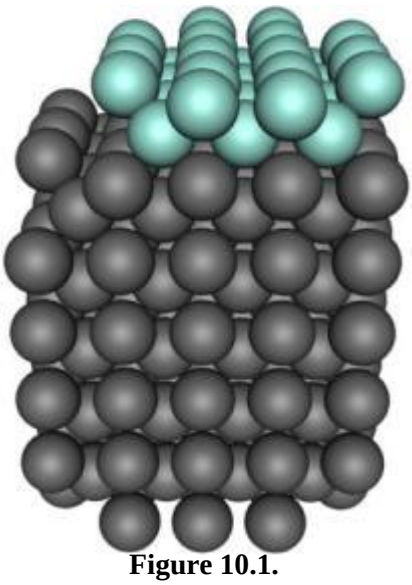

Figure 10.1.

11. BCC MODEL AND MAGIC NUMBERS

The main motivative of shell model is the unusual stability of nuclei which have number of protons or neutrons equal to magic number. BCC model can give an explanation for stability of some nuclei which have magic

number depending on the structure of these nuclei. In this model nuclei which have magic numbers 2, 8, 20, 28 have very organized shapes formed by complete layers of nucleons (protons or neutrons).

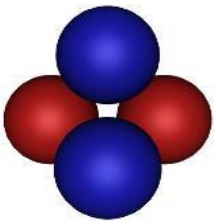

Figure 11.1. $_{2}He^{4}$.

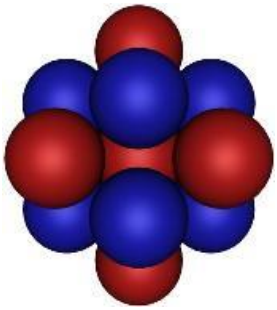

Figure 11.2. $_{7}N^{15}$.

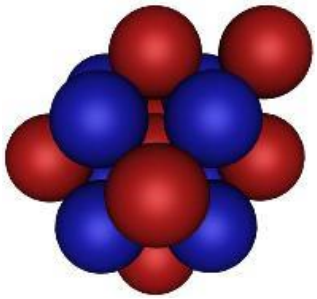

Figure 11.3. $_{8}O^{16}$ type A.

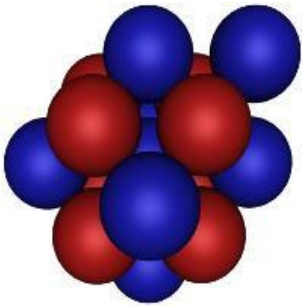

Figure 11.4. $_{8}O^{16}$ type B.

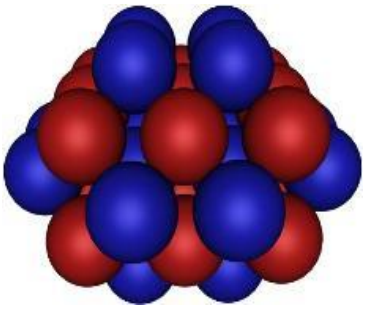

Figure 11.5. $_{18}Ar^{38}$.

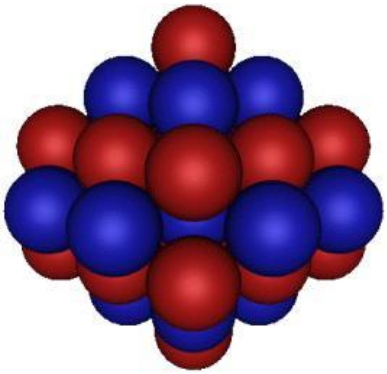

Figure 11.6. $_{20}Ca^{40}$.

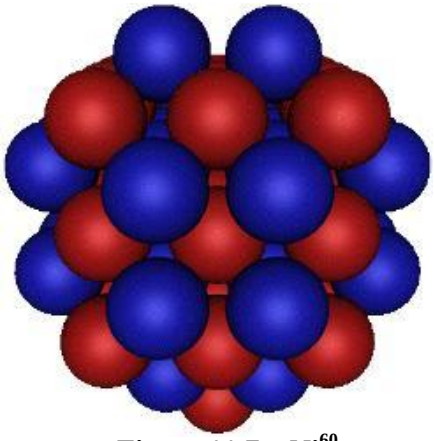

Figure 11.7. $_{28}Ni^{60}$

Also this model suggests a range of stability for nuclei have atomic number 36 , 48 , 64 , 80 as they have a structure of complete layers of protons.

12. THE NEW CONCEPT OF NUCLEAR FORCE

This model gives a new concept of nuclear force depending on the bonds between protons and neutrons. These bonds are used in calculating the nuclear binding energy.
In this model there are no bonds between similar nucleons, but only between unlike nucleons (protons and neutrons). So in this model the interaction is only between a proton and a neutron.
The energy of each interaction should equal the energy of the bond which is considered to be the constant used in calculating nuclear binding energy (about 4 MeV).

$$E_b = 4.08_{(MeV)}\, B - (0.711_{(MeV)}\, Z^2) / A^{1/3}$$

Like checker board model, the nature of this interaction is assumed to be electromagnetic.
It is known that protons and neutrons are formed from smaller particles called quarks. There are two types of quarks in nucleons:

1-upquark: which has 2/3 of the proton +ve charge.
2-downquark: which has 1/3 of the electron –ve charge.

Any solid model of nuclear structure deals with protons and neutrons as spheres and to achieve this spherical shape, it is assumed that the structure of a proton or a neutron have two orbits normal to each other and this occurs when every two identical quarks of a nucleons orbits the third quark. (Figure 12.1)

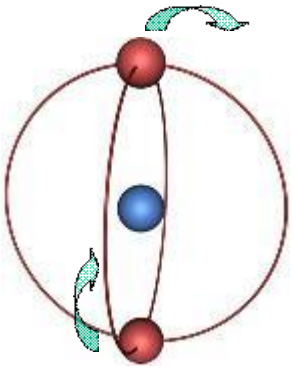

Figure 12.1. Proton. (blue down quark), (red up quark).

"Checker board model evolved out of the assumption that the two up quarks in the proton revolve around the down quark which is located in the centre of the proton. Similarly the two down quarks revolve around the up quark in the centre of the neutron. This model assumes that the strong nuclear force is generated from the close approach of the up quarks in the proton and down quarks in the neutron." [10]
“The neutron charge distribution with an inner positive charge and outer layer of negative charge is consistent with its negative magnetic moment.” [11]

In proton: there are two up quarks orbiting one down quark.
In neutron: there are two down quarks orbiting one up quark.

In BCC model the maximum number of neighbours by which each nucleon is surrounded is 8 (a proton will be surrounded by 8 neutrons and vice versa). These 8 neutrons will be distributed on the two orbits of the proton keeping the distances and angles assumed by the structure. (Figure 12.2), (Figure 12.3)

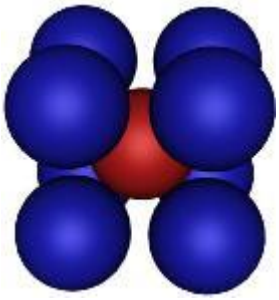

Figure 12.2.

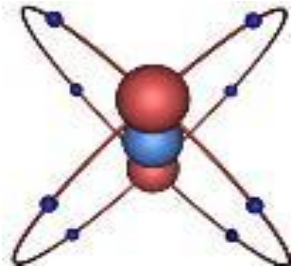

Figure 12.3.

It is clear that each touch point between the proton and a neutron will lie between one of the proton's two orbits and one of the neutron's two orbits. (Figure 12.4)

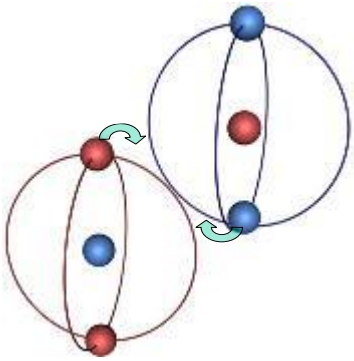

Figure 12.4.

There are two different quarks existing in the two orbits in touch with each other. The harmonious motion of these two quarks will result in net electromagnetic attraction force between the proton and the neutron.

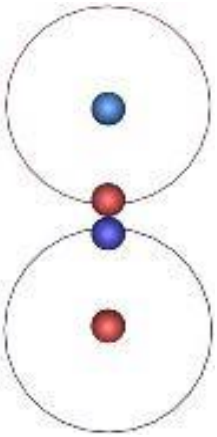

Figure 12.5.

It is clear that This assumed attraction force must undergo further more calculation to say that it could be the real nuclear force.

Simple comparison between this force and the nuclear force

It is known that nuclear force works through a very **short range** and it becomes a repulsive force at distance less than **0.4fm.**

The properties of the assumed force

1- It has a **short range** as at long distances nucleons deal with each other as electrostatic charged points for example a proton is positive point do not have effect on a neutron which is equal point but as they approach each other to a suitable distance the effect of electrostatic forces between quarks begin to appear.

2- In this model we note that the least separation distance between any two identical nucleons is **0.4217fm** and this distance is kept fixed in all nuclei as if it changed between any two nucleons, the structure loses the balance of all distances and angles between nucleons.

This assumed force has the same two properties with which nuclear force is distinguished.

So the question now is

(May this electrostatic force is the real nuclear force?).

Appendix A.

Table 1. Number of bonds for nucleus.

Element	B	B per nucleon	Element	B	B per nucleon
$_{2}He^{4}$	4	1	$_{44}Ru^{102}$	288	2.8235
$_{3}Li^{7}$	10	1.4286	$_{45}Rh^{103}$	290	2.8155
$_{4}Be^{9}$	15	1.6667	$_{46}Pd^{106}$	300	2.8302
$_{5}B^{11}$	20	1.8182	$_{47}Ag^{107}$	302	2.8224
$_{6}C^{12}$	22	1.8333	$_{48}Cd^{114}$	324	2.8421
$_{7}N^{14}$	27	1.9286	$_{49}In^{115}$	328	2.8522
$_{8}O^{16}$	34	2.125	$_{50}Sn^{120}$	340	2.8333
$_{9}F^{19}$	41	2.1053	$_{51}Sb^{121}$	344	2.843
$_{10}Ne^{20}$	44	2.2	$_{52}Te^{126}$	356	2.8254
$_{11}Na^{23}$	52	2.2609	$_{53}I^{127}$	359	2.8268
$_{12}Mg^{24}$	56	2.3333	$_{54}Xe^{132}$	375	2.8409
$_{13}Al^{27}$	64	2.3704	$_{55}Cs^{133}$	378	2.8421
$_{14}Si^{28}$	68	2.4286	$_{56}Ba^{138}$	392	2.8406
$_{15}P^{31}$	76	2.4516	$_{57}la^{139}$	398	2.8633
$_{16}S^{32}$	80	2.5	$_{58}Ce^{140}$	404	2.8857
$_{17}Cl^{35}$	88	2.5143	$_{59}Pr^{141}$	408	2.8936
$_{18}Ar^{38}$	96	2.5	$_{60}Nd^{142}$	412	2.9014
$_{19}K^{39}$	100	2.5641	$_{61}Pm^{145}$	419	2.8897
$_{20}Ca^{40}$	104	2.6	$_{62}Sa^{150}$	435	2.9000
$_{21}Sc^{45}$	116	2.5778	$_{63}Eu^{153}$	444	2.9020
$_{22}Ti^{48}$	125	2.6042	$_{64}Gd^{158}$	458	2.8987
$_{23}V^{51}$	134	2.6275	$_{65}Tb^{161}$	462	2.9057
$_{24}Cr^{52}$	138	2.6538	$_{66}Dy^{164}$	474	2.8902
$_{25}Mn^{55}$	146	2.6545	$_{67}Ho^{165}$	478	2.8970
$_{26}Fe^{56}$	150	2.6786	$_{68}Er^{166}$	483	2.9096
$_{27}Co^{59}$	160	2.7119	$_{69}Tm^{169}$	491	2.9053
$_{28}Ni^{60}$	164	2.7333	$_{70}Yb^{174}$	504	2.8966
$_{29}Cu^{63}$	172	2.7302	$_{71}Lu^{175}$	507	2.8971
$_{30}Zn^{64}$	174	2.7188	$_{72}Hf^{180}$	519	2.8833

$_{31}Ga^{69}$	189	2.7391
$_{32}Ge^{74}$	202	2.7297
$_{33}As^{75}$	205	2.7333
$_{34}Se^{80}$	220	2.75
$_{35}Br^{81}$	224	2.7654
$_{36}Kr^{80}$	224	2.8
$_{36}Kr^{84}$	232	2.7619
$_{37}Rb^{85}$	236	2.7765
$_{38}Sr^{88}$	244	2.7727
$_{39}Y^{89}$	248	2.7865
$_{40}Zr^{90}$	252	2.8
$_{41}Nb^{93}$	260	2.7957
$_{42}Mo^{98}$	274	2.7959
$_{73}Ta^{181}$	524	2.8950
$_{74}W^{184}$	532	2.8913
$_{75}Re^{187}$	541	2.8930
$_{76}Os^{190}$	552	2.9053
$_{77}Ir^{193}$	561	2.9067
$_{78}Pt^{195}$	569	2.9179
$_{79}Au^{197}$	575	2.9188
$_{80}Hg^{202}$	592	2.9307
$_{81}Tl^{205}$	600	2.9268
$_{82}Pb^{208}$	608	2.9231
$_{83}Bi^{209}$	612	2.9282
$_{90}Th^{232}$	663	2.8578
$_{92}U^{238}$	682	2.8655

Appendix B.

Table 2. Number of bonds versus $\left(E_b + (0.711_{(MeV)}\, Z^2) / A^{1/3}\right)$.

Element	B	E_b	Cloumb effect	Sum
$_{2}He^{4}$	4	28.3	1.7916	30.0916
$_{3}Li^{7}$	10	39.25	8.4291	47.6791
$_{4}Be^{9}$	15	58.17	5.4690	63.639
$_{5}B^{11}$	20	76.21	7.9924	84.2024
$_{6}C^{12}$	22	92.16	11.1801	103.3401
$_{7}N^{14}$	27	104.66	14.4552	119.1152
$_{8}O^{16}$	34	127.62	18.0583	145.6783
$_{9}F^{19}$	41	147.8	21.5823	169.3823
$_{10}Ne^{20}$	44	160.65	26.1935	186.8435
$_{11}Na^{23}$	52	186.57	30.2514	216.8214
$_{12}Mg^{24}$	56	198.26	35.4946	233.7546
$_{13}Al^{27}$	64	224.95	40.0530	265.003
$_{14}Si^{28}$	68	236.54	45.8923	282.4323
$_{15}P^{31}$	76	262.92	50.9251	313.8451
$_{16}S^{32}$	80	271.78	57.3314	329.1114
$_{17}Cl^{35}$	88	298.21	62.8171	361.0271
$_{18}Ar^{38}$	96	327.35	68.5204	395.8704
$_{19}K^{39}$	100	333.72	75.0511	408.7711
$_{20}Ca^{40}$	104	342.06	83.1591	425.2191
$_{21}Sc^{45}$	116	387.86	88.1531	476.0131
$_{22}Ti^{48}$	125	418.7	94.6894	513.3894
$_{23}V^{51}$	134	445.85	101.4227	547.2727
$_{24}Cr^{52}$	138	456.35	109.7213	566.0713
$_{25}Mn^{55}$	146	482.08	116.8500	598.93
$_{26}Fe^{56}$	150	492.26	125.6281	617.8881
$_{27}Co^{59}$	160	517.32	133.1414	650.4614
$_{28}Ni^{60}$	164	526.85	142.3864	669.2364
$_{29}Cu^{63}$	172	551.39	150.2745	701.6645
$_{30}Zn^{64}$	174	559.10	159.975	719.075
$_{31}Ga^{69}$	189	602.00	166.5878	768.5878

$_{32}Ge^{74}$	202	645.68	173.4173	819.0973
$_{33}As^{75}$	205	652.58	183.6019	836.1819
$_{34}Se^{80}$	220	696.88	190.7498	887.6298
$_{35}Br^{81}$	224	704.38	201.3001	905.6801
$_{36}Kr^{80}$	224	695.44	213.8510	909.291
$_{36}Kr^{84}$	232	732.27	210.4012	942.6712
$_{37}Rb^{85}$	236	739.29	221.3775	960.6675
$_{38}Sr^{88}$	244	768.47	230.8213	999.2913
$_{39}Y^{89}$	248	775.55	242.2156	1017.766
$_{40}Zr^{90}$	252	783.90	253.8490	1037.749
$_{41}Nb^{93}$	260	805.78	263.8009	1069.581
$_{42}Mo^{98}$	274	846.26	272.0359	1118.296
$_{44}Ru^{102}$	288	877.96	294.6060	1172.566
$_{45}Rh^{103}$	290	884.18	307.1488	1191.329
$_{46}Pd^{106}$	300	909.49	317.8947	1227.385
$_{47}Ag^{107}$	302	915.28	330.8294	1246.109
$_{48}Cd^{114}$	324	972.61	343.9887	1316.599
$_{49}In^{115}$	328	963.10	351.0447	1314.145
$_{50}Sn^{120}$	340	1020.6	360.3705	1380.971
$_{51}Sb^{121}$	344	1026.3	373.8937	1400.194
$_{52}Te^{126}$	356	1066.4	383.4889	1449.889
$_{53}I^{127}$	359	1072.6	397.3319	1469.932
$_{54}Xe^{132}$	375	1112.5	407.1919	1519.692
$_{55}Cs^{133}$	378	1118.6	421.3514	1539.951
$_{56}Ba^{138}$	392	1158.3	431.4720	1589.772
$_{57}la^{139}$	398	1164.6	445.9447	1610.545
$_{58}Ce^{140}$	404	1172.7	460.6272	1633.327
$_{59}Pr^{141}$	408	1177.9	475.5183	1653.418
$_{60}Nd^{142}$	412	1185.2	490.6171	1675.817
$_{61}Pm^{145}$	419	1203.9	503.5856	1707.486
$_{62}Sa^{150}$	435	1239.3	514.3861	1753.686
$_{63}Eu^{153}$	444	1259.0	527.6188	1786.619
$_{64}Gd^{158}$	458	1295.9	538.6961	1834.596
$_{65}Tb^{161}$	462	1302.1	554.4945	1856.595
$_{66}Dy^{164}$	474	1338.1	565.8173	1903.917
$_{67}Ho^{165}$	478	1344.3	581.9128	1926.213
$_{68}Er^{166}$	483	1351.6	598.2069	1949.807
$_{69}Tm^{169}$	491	1371.4	612.2642	1983.664
$_{70}Yb^{174}$	504	1406.6	624.0450	2030.645
$_{71}Lu^{175}$	507	1418.4	640.7770	2059.177
$_{72}Hf^{180}$	519	1446.3	652.7954	2099.095
$_{73}Ta^{181}$	524	1452.3	669.8164	2122.116
$_{74}W^{184}$	532	1473.0	684.5320	2157.532
$_{75}Re^{187}$	541	1491.9	699.3774	2191.277
$_{76}Os^{190}$	552	1526.2	714.3520	2240.552
$_{77}Ir^{193}$	561	1532.1	729.4552	2261.555
$_{78}Pt^{195}$	569	1545.7	745.9572	2291.657
$_{79}Au^{197}$	575	1559.4	762.6086	2322.009
$_{80}Hg^{202}$	592	1595.2	814.7921	2409.992
$_{81}Tl^{205}$	600	1615.1	791.1431	2406.243
$_{82}Pb^{208}$	608	1636.5	806.8812	2443.381

$_{83}Bi^{209}$	612	1640.3	825.3605	2465.661
$_{90}Th^{232}$	663	1766.7	937.2569	2703.957
$_{92}U^{238}$	682	1801.7	971.0754	2772.775

References:

[1] L. R. Hafstad and E. Teller, Phys. Rev. **54**, 681 (1938)
[2] E. Feenberg, Rev. Mod. Phys. **19**, 239 (1947)
[3] M.G. Mayer, Phys. Rev. **75**, 1969 (1949)
[4] J. Garai: Double Tetrahedron structure of the nucleus (http://lanl.arxiv.org/abs/nucl-th/0309035)
[5] S. D. Schery, D. A. Lind, and C. D. Zafiratos, Phys. Lett. B **97**, 25 (1980)
[6] N.D. Cook (k9.physics.indiana.edu/~eric/QNP/QNP/QNP_2004_talks/session1_Monday/N_Cook.ppt).
[7] L. Pauling, Science 150 297 (1965)
L. Pauling, Phys. Rev. Lett. 15 499 (1965)
L. Pauling Research Notebooks 25,26 (http://osulibrary.orst.edu/specialcollections/rnb/index.html)
[8] N.D. Cook and T. Hayashi, J. Phys. G: Nucl. Phys. **23** 1109 (1997)
N.D. Cook, Proceedings of the St. Andrews Conf. on Fission (Singapore: World Scientific) p 217 (1999)
[9] H. Kondo and M. Uehara Progress of Theoretical Physics 70 1307 (1983)
[10]T. M. Lach, Checker board model (http://meetings.aps.org/link/BAPS.2007.APR.X16.6)
[11]F. Yang and J. H. Hamilton, Modern Atomic and Nuclear Physics. McGraw-Hill p687 (1996)
[12] T. Goldman, K. R. Maltman, Jr. G. J. Stephenson and K. E. Schmidt, Nuclear Phys. **481** 621 (1988)